



High strength and ductility of friction-stir-welded steel joints due to mechanically stabilized metastable austenite

Hidetoshi Fujii,^{a,*} Rintaro Ueji,^a Yoshiaki Morisada^a and Hiroyasu Tanigawa^b

^aJoining and Welding Research Institute, Osaka University, 11-1, Mihogaoka, Ibaraki, Osaka 567-0047, Japan

^bJapan Atomic Energy Agency, 2-166, Obuchi-Omotodate, Rokkasho, Aomori 039-3212, Japan

Received 31 August 2013; revised 9 September 2013; accepted 10 September 2013

Available online 18 September 2013

Steel plates were friction-stir-welded together under conditions in which samples were first heated above the lower critical temperature of the alloy and subsequently cooled at approximately 100 K s^{-1} . This method produced joints with an excellent balance between tensile strength and ductility. Severe plastic deformation during friction-stir-welding stabilized the austenite phase in the steel joints. The austenite phase was subsequently transformed through deformation into the martensite phase when the joints were actually used.

© 2013 Acta Materialia Inc. Published by Elsevier Ltd. All rights reserved.

Keywords: Friction stir welding; Steels; Mechanical properties; Microstructure; Phase transformation

Welding and joining are multibillion-dollar fabrication technologies extensively used in the construction, transport, aerospace, energy, shipbuilding and electronics industries [1]. However, the material properties of steel generally deteriorate as steel parts are welded and joined together. Accordingly, there have previously been numerous attempts to minimize the deterioration of the mechanical properties of steel joints. We demonstrate for the first time ever that friction-stir-welding (FSW) can produce a mechanically stabilized metastable austenite phase that actually increases the elongation and tensile strength of steel joints.

FSW is a revolutionary method of solid-state joining that was invented in the UK [2]. In FSW, a 10–20 mm diameter rod-like tool rotating at high speed is pressed onto the surface of the material to be joined where it generates frictional heat. The tool is then moved along the interface of the material to join parts together. Because the maximum temperature of FSW is below the melting point of the material, joints produced using FSW exhibit material properties that are superior to those of the base metal. Therefore, FSW has recently been used for a wide variety of low-melting-point materials such as Al, Mg and Cu alloys [3–12]. Application of FSW to various steels has become possible through the

development of appropriate tools and because of work that has been done to determine the appropriate welding conditions [13–22].

Several of the authors have previously used FSW to develop a method of welding together plain carbon steel parts below the lower critical temperature, A_{C1} (726 °C), of carbon steel [19–21]. A joint without a martensite structure is produced even when the method is used to weld together parts produced with hypereutectoid steel (0.85 wt.% C, AISI-1080). Such steel is very difficult to weld using conventional methods of welding because phase transformation causes cracks to form in the steel. However, the authors believed that a method of welding such as FSW, which does not induce phase transformation, could be used to weld such steel while retaining the toughness of welded high-carbon steel joints. Joints produced using the method they developed exhibited mechanical properties that are superior to those of joints produced using conventional methods of welding. When the method was extended to welding other difficult-to-weld metals, we found that although the austenite phase in steel is completely unstable at room temperature, FSW significantly stabilizes the austenite phase against the martensite reaction at room temperature, which is an interesting and completely unexpected phenomenon.

The chemical composition of the steel alloy used in this study was 0.1 C, 8 Cr, 2 W, 0.2 V, 0.04 Ta (wt.%), and the balance was Fe. This steel consists of

* Corresponding author. Tel./fax: +81 6 6879 8643; e-mail: fujii@jwri.osaka-u.ac.jp

ferrite and tempered martensite phases and can be categorized as high-chromium ferritic steel. The A_{C1} temperature of this alloy is 850 °C based on dilatometry. High-chromium steel is difficult to weld because of the precipitation of brittle phases, which is why the authors selected this particular steel for this study. FSW was conducted under the following conditions: the rotating tool was made of cemented carbide (i.e. tungsten carbide, WC), which has high strength, high toughness and good thermal conductivity in the range of welding temperatures anticipated in this study. The tool had a 12 mm diameter shoulder and a probe 4 mm in diameter and 1.4 mm long was used at a tilt of 3° from the normal to the plate. FSW was performed at rotational speeds of 100–300 rpm and at a constant welding speed of 100 mm min⁻¹. Argon was used as a shielding gas at a flow rate of 30 l min⁻¹ to prevent oxidation of the steel and the tool during FSW.

Frigaard et al. [23] reported that the total amount of heat generated during FSW, q_0 , can be given by the following equation:

$$q_0 = \int_0^R 4\pi^2 \mu P N r^2 dr = \frac{4}{3} \pi^2 \mu P N R^3, \quad (1)$$

where μ is the friction coefficient, R (m) is the surface radius, N (s⁻¹) is the rotation speed and P (N m⁻³) is the mean pressure at the interface between the tool and joint. Eq. (1) can be used to control heat generation by varying N while fixing μ , P and R , i.e. more heat is input into a joint with increasing N .

The mechanical properties of the joints welded together at each N were assessed by tensile testing at a quasi-static strain rate. In addition, the macrostructures of cross-sections of the joint cut perpendicular to the FSW direction were observed by optical microscopy and scanning electron microscopy (SEM) using a microscope equipped with an electron backscatter diffraction (EBSD) detector. Each cross-section was polished to a mirror finish and was then etched using Keller's solution (95% HNO₃ + 1% C₂H₅OH + 1.5% HF + 2.5% HCl).

Figure 1 shows the microstructures of cross-sections of the joints welded together at each N . Defect-free joints were obtained at each N . The welding temperature was above the A_{C1} transformation point when $N = 300$ rpm and the stir zone whitened, indicating the formation of a phase distinguishable from the one that had formed below A_{C1} and that was indicated by a

Rotation speed (rpm)	Welding speed (mm/min)	RS	Cross-Section	AS
100	100			
200	100			
300	100			

Figure 1. Cross-sections of joints welded at various rotation speeds and at a constant welding speed of 100 mm min⁻¹. At a rotation speed of 100 rpm, the entire stir zone was dark white and was formed at temperature below A_{C1} . At rotation speed of 300 rpm, however, the stir zone was white when formed at a temperature above A_{C1} . At a rotation speed of 200 rpm, the welding temperature was above A_{C1} in the upper part of stir zone and below A_{C1} in the lower part.

peripheral dark area. When $N = 200$ rpm, the welding was performed above A_{C1} from the top to the middle of the stir zone and below A_{C1} from the middle to the bottom of the stir zone. Accordingly, the boundary between the white and dark areas is observed in the central part of the stir zone. When $N = 100$ rpm, on the other hand, the entire stir zone was formed below A_{C1} , and no such boundary was observed.

The maximum welding temperatures were measured at the centre back surfaces of the butt samples. The temperatures were 740, 762, and 787 °C when $N = 100$, 200, and 300 rpm, respectively. The maximum welding temperature was below the A_{C1} temperature when $N = 100$ and 200 rpm, and above it when $N = 300$ rpm. The cooling rate decreased with increasing rotation speed. When the cooling rate is defined as the average cooling rate from the maximum temperature to 500 °C, the cooling rate was 58, 78 and 120 °C s⁻¹ when $N = 100$, 200 and 300 rpm, respectively. FSW was performed in the single- γ phase or ($\alpha + \gamma$) phase temperature regions when $N = 300$ rpm. When $N = 100$ rpm, on the other hand, it was performed without any phase transformation. However, the temperature was measured at the bottom of the plates; therefore, it is necessary to examine the microstructure to determine whether the phase actually transforms during FSW.

Figure 2 shows the phase maps obtained for the central part of the stir zone by measuring the EBSD of the joints when $N = 100$ –300 rpm. There is a microstructure boundary at the centre of the stir zone when $N = 200$ rpm, as previously mentioned. Accordingly, the phase maps for both the upper and lower parts of the stir zone are shown. Body-centred cubic (bcc) ferrite

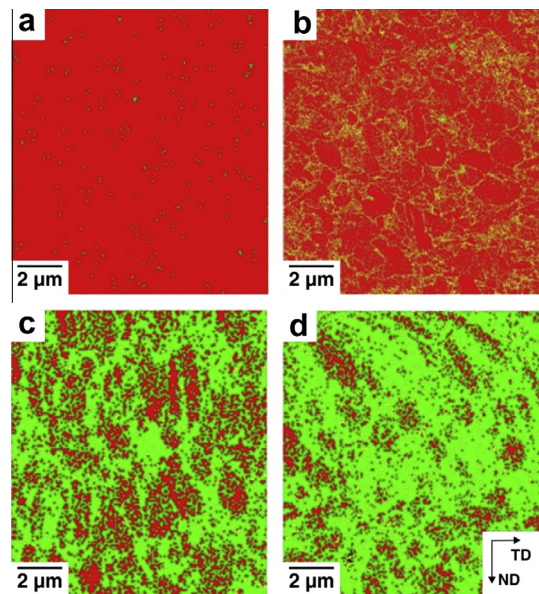


Figure 2. Phase maps for joints friction-stir-welded at rotation speeds of (a) 100, (b) 200 (lower stir zone), (c) 200 (upper stir zone) and (d) 300 rpm. Red and green indicate ferrite and austenite phases, respectively, and yellow points denote locations where phase cannot be precisely determined. (For interpretation of the references to colour in this figure legend, the reader is referred to the web version of this article.)

phases are observed in the phase map obtained when $N = 100$ rpm. When $N = 300$ rpm, on the other hand, the face-centred cubic (fcc) austenite phase retained in the joint is observed in the phase map, which is completely different from the phases observed in the phase map for the continuously cooled microstructure, i.e. the ferrite and martensite phases are simultaneously formed in the continuously cooled microstructure without any deformation even at the same cooling rate.

The new finding in this study is that although the austenite phase in steel is completely unstable at room temperature, FSW significantly stabilizes the austenite phase against the martensite reaction at room temperature, while the martensite start temperature of this alloy is $400\text{ }^{\circ}\text{C}$ measured by dilatometry. The stabilization of the austenite phase seems to be due to the significant plastic deformation of that phase during FSW. Plastic deformation creates a high density of dislocations, which increases the magnitude of the internal stress of the austenite phase. The martensite transformation, on the other hand, requires long-range movement of the interface under the stress, τ_T , which originates from the change in chemical free-energy, ΔG , of the transformation as follows [24,25]:

$$\tau_T = \phi \Delta G, \quad (2)$$

where ϕ is a constant, and ΔG is the difference between the free energies of the ferrite, G_{α} , and austenite, G_{γ} , phases, i.e. $\Delta G = G_{\gamma} - G_{\alpha}$. The martensite transformation does not occur when the magnitude of the internal stress exceeds τ_T during FSW; thus, the austenite phase should be retained in the steel. It should also be noted that the cooling rate of the phases in the stir zone is generally much higher ($\sim 100\text{ K s}^{-1}$) than that of those in practical heat treatment processes such as hot rolling adopted in the steel industry, and that this condition helps prevent diffusional transformation and dislocation annihilation.

All the welded joints were then broken at the base metal to obtain standard tensile specimens whose gauge parts included both the stir zone and the base metal. From these, only the tensile specimens whose gauge part was exclusively composed of the stir zone were prepared. The gauge width and length were 3 and 2 mm, respectively. Figure 3 shows the stress–strain curves obtained for the three joints and for the base metal. Because the welding was completed without any phase transformation when $N = 100$ rpm, the tensile strength of the joint was similar to that of the base metal. For the welding completed when $N = 200$ or 300 rpm, on the other hand, the tensile strength of the joints was significantly higher than that of the base material. Note that the elongation of these joints was also higher than that of the base material.

When $N = 300$ rpm, the welding was performed in the $(\alpha + \gamma)$ phase or the single-phase γ -phase temperature range for the entire stir zone, and the austenite phase was retained in the steel because of severe plastic deformation during FSW. The retained austenite phase was then transformed into the martensite phase through the well-known transformation-induced plasticity (TRIP) effect [26] during the tensile test. As a result, the elongation and tensile strength of the joint were sig-

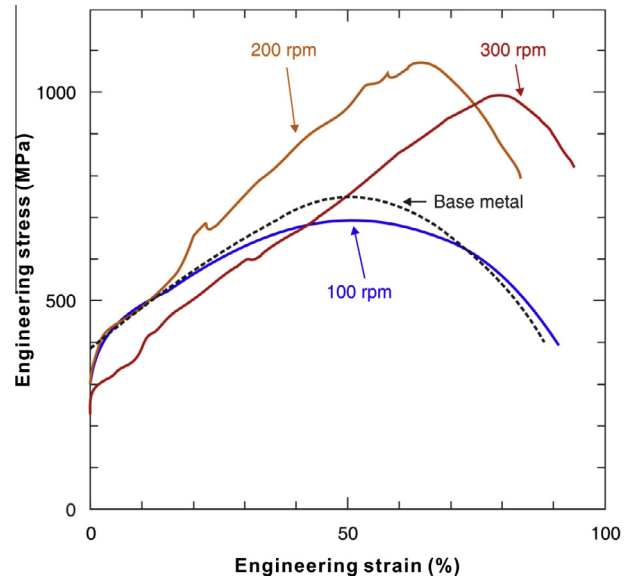


Figure 3. Stress–strain curves for stir zones in joints produced using FSW. Data for base metal are denoted by a dotted line for reference. Because austenite phase retained in joints produced at rotation speeds of 200 or 300 rpm was transformed into martensite phase during tensile test, the elongation and tensile strength of joints was significantly higher than those of base metal. FSW conveys these excellent properties to steel through formation of mechanically stabilized metastable austenite phase.

nificantly higher than those of the base metal. Although the TRIP effect is expected for steel alloys produced with a special chemical composition that promotes TRIP, FSW induces the TRIP effect for steel alloys that are not produced with the special chemical composition.

When $N = 200$ rpm, the retained austenite phase was obtained in the upper part of the stir zone after the FSW, whereas the ferrite phase was retained in the lower part during the FSW due to the lower peak temperature, which was not high enough for the transformation to the austenite phase. This constitution of the microstructure was strongly related to its tensile properties. The joint produced when $N = 200$ rpm exhibited higher tensile strength than the one produced when $N = 300$ rpm. In particular, the yield stress of the former was higher than that of the latter because the former consists of the bcc ferrite phase in the bottom part of the stir zone and the fcc austenite phase in the upper part and because the bcc ferrite phase should exhibit higher yield strength than the fcc austenite phase. The elongation of the joint produced when $N = 300$ rpm, on the other hand, is higher than that of the joint produced when $N = 200$ rpm because the former consisted almost entirely of the retained austenite phase.

FSW of a steel alloy was performed at a welding speed of 100 mm min^{-1} and at various rotation speeds in the range 100–300 rpm, some of which induced martensite phase transformation and others of which did not. Under these welding conditions, the welding temperature can be easily controlled above and below A_{C1} during welding by controlling the rotation speed. On the basis of these results, it was concluded that deformation of the austenite phase enhances its stability against the martensite reaction.

Accordingly, FSW enables the production of joints with an excellent balance between tensile strength and ductility because of the formation of the mechanically stabilized metastable austenite phase. The metastable austenite phase retained in the steel was transformed into the martensite phase when deformation was induced in a welded structure at room temperature. Consequently, both the tensile strength and elongation of the joints produced using FSW were significantly higher than those of the base material.

The authors wish to acknowledge the financial support of a Collaborative Research Based on Industrial Demand by Japan Science and Technology Agency (JST), the Global COE Programs from the Ministry of Education, Sports, Culture, Science, a Grant-in-Aid for Science Research from the Japan Society for Promotion of Science and Technology of Japan, and the Japan Atomic Energy Agency Joint Work System.

- [1] S.A. David, T. DebRoy, *Science* 257 (497–502) (1992) 497.
- [2] W.M. Thomas, E.D. Nicholas, J.C. Needham, M.G. Murch, P. Temple-Smith, C.J. Dawes, International Patent Application No. PCT/GB92/02203.
- [3] R.S. Mishra, Z.Y. Ma, *Mater. Sci. Eng., R* 50 (2005) 1.
- [4] R.S. Mishra, M.W. Mahoney, *Friction Stir Welding and Processing*, ASM International, Materials Park, OH, 2007.
- [5] R. Nandan, T. DebRoy, H.K.D.H. Bhadeshia, *Prog. Mater. Sci.* 53 (2008) 980.
- [6] H. Okamura, K. Aota, M. Ezumi, *J. Jpn. Inst. Light Met.* 50 (2000) 166.
- [7] G. Campbell, T. Stotler, *Weld. J.* 78 (1999) 45.
- [8] M.R. Johnsen, *Weld. J.* 78 (1999) 35.
- [9] K. Colligan, *Weld. J.* 78 (1999) 229.
- [10] K.E. Knipstron, B. Pekkari, *Weld. J.* 76 (1997) 55.
- [11] C.J. Dawes, W.M. Thomas, *Weld. J.* 75 (1996) 41.
- [12] Y. Morisada, H. Fujii, Y. Kawahito, K. Nakata, M. Tanaka, *Scripta Mater.* 65 (2011) 1085.
- [13] W.M. Thomas, P.L. Threadgill, E.D. Nicholas, *Sci. Technol. Weld. Joining* 4 (1999) 365.
- [14] T.J. Lienert, W.L. Stellwag, B.B. Grimmett, R.W. Warke, *Weld. J.* 82 (2003) 1s.
- [15] A.P. Reynolds, W. Tang, T. Guaupel-Herold, H. Prask, *Scripta Mater.* 48 (2003) 1289.
- [16] P.J. Konkol, C.J.A. Mathers, R. Johnson, J.R. Pickens, *J. Ship Prod.* 19 (2003) 159.
- [17] S.H.C. Park, Y.S. Sato, H. Kokawa, K. Okamoto, S. Hirano, M. Inagaki, *Scripta Mater.* 49 (2003) 1175.
- [18] R. Ueji, H. Fujii, L. Cui, A. Nishioka, K. Kunishige, K. Nogi, *Mater. Sci. Eng., A* 423 (2006) 324.
- [19] H. Fujii, L. Cui, N. Tsuji, M. Maeda, K. Nakata, K. Nogi, *Mater. Sci. Eng., A* 429 (2006) 50.
- [20] L. Cui, H. Fujii, N. Tsuji, K. Nogi, *Scripta Mater.* 56 (2007) 637.
- [21] Y.D. Chung, H. Fujii, R. Ueji, N. Tsuji, *Scripta Mater.* 63 (2010) 223.
- [22] M. Ghosh, K. Kumar, R.S. Mishra, *Scripta Mater.* 63 (2010) 851.
- [23] Ø. Frigaard, Ø. Grong, O.T. Midling, *Metall. Mater. Trans. A* 32 (2001) 1189.
- [24] G.B. Olson, M.A. Cohen, *Metall. Trans. A* 7 (1976) 1897.
- [25] S. Chatterjee, H.-S. Wang, J.R. Yang, H.K.D.H. Bhadeshia, *Mater. Sci. Technol.* 22 (2006) 641.
- [26] J. Angle, *J. Iron Steel Inst.* 177 (1954) 165.